0013-7227/06/$15.00/0
Printed in U.S.A.

Endocrinology 147(9):4067–4078

doi: 10.1210/en.2005-1536

Peroxisome Proliferator-Activated Receptor-α-Null Mice Have Increased White Adipose Tissue Glucose Utilization, GLUT4, and Fat Mass: Role in Liver and Brain

Claude Knauf, Jennifer Rieusset, Marc Foretz, Patrice D. Cani, Marc Uldry, Masaya Hosokawa, Estelle Martinez, Matthieu Bringart, Aurélie Waget, Sander Kersten, Béatrice Desvergne, Sandrine Gremlich, Walter Wahli, Josiane Seydoux, Nathalie M. Delzenne, Bernard Thorens, and Rémy Burcelin

Unité Mixté de Recherche 5018 (C.K., P.D.C., E.M., M.B., A.W., R.B.), Centre National de la Recherche Scientifique, University Paul Sabatier, 31403 Toulouse, France; Institut de Biologie Animale (J.R., S.K., B.D., S.G., W.W.), Université de Lausanne, CH-1015 Lausanne, Switzerland; Département de Physiologie (J.S.), Faculté de Médecine, Université de Genève, CH-1211 Genève, Switzerland; Institut de Pharmacologie et de Toxicologie (M.F., M.U., M.H., B.T.), Université de Lausanne, CH-1005 Lausanne, Switzerland; and Unit of Pharmacokinetics, Metabolism, Nutrition, and Toxicology (P.D.C., N.M.D.), Université Catholique de Louvain, B-1348 Brussels, Belgium

Activation of the peroxisome proliferator-activated receptor (PPAR)-α increases lipid catabolism and lowers the concentration of circulating lipid, but its role in the control of glucose metabolism is not as clearly established. Here we compared PPARα knockout mice with wild type and confirmed that the former developed hypoglycemia during fasting. This was associated with only a slight increase in insulin sensitivity but a dramatic increase in whole-body and adipose tissue glucose use rates in the fasting state. The white sc and visceral fat depots were larger due to an increase in the size and number of adipocytes, and their level of GLUT4 expression was higher and no longer regulated by the fed-to-fast transition. To evaluate whether these adipocyte deregulations were secondary to the absence of PPARα from liver, we reexpresssed this transcription factor in the liver of knockout mice using recombinant adenoviruses. Whereas more than 90% of the hepatocytes were infected and PPARα expression was restored to normal levels, the whole-body glucose use rate remained elevated. Next, to evaluate whether brain PPARα could affect glucose homeostasis, we activated brain PPARα in wild-type mice by infusing WY14643 into the lateral ventricle and showed that whole-body glucose use was reduced. Hence, our data show that PPARα is involved in the regulation of glucose homeostasis, insulin sensitivity, fat accumulation, and adipose tissue glucose use by a mechanism that does not require PPARα expression in the liver. By contrast, activation of PPARα in the brain stimulates peripheral glucose use. This suggests that the alteration in adipocyte glucose metabolism in the knockout mice may result from the absence of PPARα in the brain. (*Endocrinology* 147: 4067–4078, 2006)

PEROXISOME PROLIFERATOR-ACTIVATED receptors (PPARs)-α, -β, and -γ are fatty acid-activated nuclear transcription factors that control numerous genes involved in lipid metabolism (1, 2). The PPARα isoform is expressed mostly in tissues with high rates of fatty acid oxidation and peroxisomal metabolism (3), such as brown fat, liver, glial cells of the brain, and heart (4–6). Whereas the role of PPARα has been studied in several tissues, its function in the control of glucose homeostasis remains unclear.

In the presence of fatty acids, fibrates, and peroxisome proliferators, PPARα triggers the expression of hepatic genes controlling fatty acid uptake, mitochondrial and peroxisomal β-oxidation, and lipoprotein assembly (7–10). Consequently, up-regulated expression of PPARα during the postabsorptive phase and fasting (9) promotes hepatic degradation of free fatty acids. This mechanism is thought to be of major importance in providing energy and to supply coenzymes for gluconeogenesis. Because during fasting the liver is the main organ producing glucose for the rest of the body, a functional gluconeogenic pathway is an important requirement for the maintenance of euglycemia. In agreement with this observation is the fact that fasted PPARα null mice develop hypoglycemia and have lower hepatic glycogen stores (11). However, the causal role of PPARα in the liver on the regulation of glucose production and maintenance of normal glycemia has not been demonstrated *in vivo*.

PPARα is also expressed in muscles in which its function is also related to increased fatty acid oxidation (12, 13) and mitochondrial metabolism. With regard to the important role of free fatty acids in insulin resistance (14, 15), one could suggest that PPARα might be an important factor in the regulation of insulin action and lipid storage. However, this putative role is controversial. Treatment with fibrate analogs improves insulin sensitivity in animal models of insulin resistance (16). Conversely, genetic ablation of PPARα had no effect on insulin resistance induced by a high-fat diet (17, 18),

First Published Online June 15, 2006

Abbreviations: ACC, Acetyl-coenzyme A carboxylase; AgRP, agouti-related protein; CART, cocaine amphetamine regulatory transcript; D-(^{3}H)-2DG, D-(^{3}H)-2-deoxyglucose; DMSO, dimethyl sulfoxide; EGP, endogenous glucose production rate; FAS, fatty acid synthase; GFP, green fluorescent protein; HKII, hexokinase II; NPY, neuropeptide Y; POMC, proopiomelanocortin; PPAR, peroxisome proliferator-activated receptor; RT, reverse transcription.

***Endocrinology* is published monthly by The Endocrine Society (http://www.endo-society.org), the foremost professional society serving the endocrine community.**

nor was insulin sensitivity improved (19). This discrepancy could be related to an incomplete analysis of the phenotype, in which not enough parameters have been characterized to fully interpret the data. Hence, further studies are required.

A third important regulatory organ expressing PPARα is the brain (20). Over recent years a considerable number of studies have shown the importance of the brain-to-peripheral tissue axis in the regulation of glucose homeostasis. It has been reported that activation of PPARα in the brain increased the expression of genes involved in free fatty oxidation and ketogenesis (21–24). This effect could be attributed to the expression of PPARα in glial cells (25) in which it could exert an antiinflammatory effect. With regard to the important physiological consequences of the control of lipid oxidation (22) and inflammation (26) in the brain, one can speculate that cerebral PPARα would be a key regulator of glucose homeostasis.

We addressed the role of PPARα in the whole body, liver, and brain on the control of whole-body glucose metabolism by assessing endogenous glucose production, tissue-specific glucose clearance rates, insulin sensitivity, and fat mass distribution and characteristics in PPARα null mice, null mice infected with a PPARα-expressing adenovirus, and mice with a PPARα activator infused into the brain. We showed that GLUT4 was overexpressed in the adipose fat pads of the knockout mice, and this was associated with an increase in fat mass, glucose use rate, and insulin hypersensitivity, which could not be reversed by reexpressing PPARα in the liver. Conversely, the chronic infusion of a PPARα activator into the brain reduced whole-body glucose use, suggesting that the impaired glucose homeostasis was dependent on PPARα expression in the brain. Moreover, in the fed state, the concentration of mRNA for neuropeptide Y (NPY) and proopiomelanocortin (POMC) was increased in the hypothalamus of PPARα knockout mice, whereas the fasting-to-fed transition was not accompanied by a normal regulation of NPY and the cocaine amphetamine regulatory transcript (CART).

Materials and Methods

Animals

Twelve to 14-wk-old wild-type C57BL/6 (Charles River, l'Arbresles, France) and PPARα-null female mice of the C57BL/6 strain were used. They were housed with an inverted dark light cycle from 0800 to 2000 h. Mice were studied in the fed state at 1400 h. For experiments in the fasting state, food was removed at 0800 h, and the mice were kept in a new clean cage for the period of time indicated. All animal experimental procedures were approved by the Rangueil Hospital Committee of the Rangueil Hospital, Toulouse, France.

Glucose turnover studies

Under anesthesia (Fluothane), an indwelling catheter was introduced into the femoral vein of mice, sealed under the back skin, and glued on the top of the skull (27). The mice were allowed to recover for 4–6 d, and they showed normal body weight and feeding behavior. The whole-body glucose use rate was determined in basal and hyperinsulinemic euglycemic conditions in 6 h fasted mice. In the basal state, HPLC purified D-(^{3}H)3-glucose (PerkinElmer, Courtaboeuf, France) was continuously infused through the femoral vein at a rate of 10 μCi/kg·min for 3 h. Under hyperinsulinemic conditions, insulin was infused at a rate of 18 mU/kg·min for 3 h. To ensure a sufficient enrichment of the plasma with D-(^{3}H)3-glucose, the tracer was infused at 30 μCi/kg·min. Plasma glucose concentrations and D-(^{3}H)3-glucose-specific activity were determined in 5 μl of blood sampled from the tip of the tail vein every 10 min during the last hour of the infusions. Throughout the infusion period, blood samples (2.5 μl) were collected from the tip of the tail vein to measure glycemia using a blood glucose meter (Roche Diagnostic, Meylan, France). Euglycemia was maintained by periodically adjusting the infusion rate of a 16.5% (wt/vol) glucose solution.

Glucose release from isolated hepatocytes

Livers from mice fasted overnight were perfused through the vena cava with a collagenase buffer as previously described (28, 29). Briefly, the isolated hepatocytes were preincubated for 2 h at 37 C in DMEM without glucose and containing pyruvate (1 mM), lactate (10 mM), and isobutylmethylxanthine (250 μM, Sigma, St. Louis, MO). The cells were then washed and incubated with the same medium also containing 0.05 μCi of ^{14}C-pyruvate (PerkinElmer). Thirty minutes later the supernatant was collected, and the ^{14}C-glucose produced was quantified after separation on ion exchange resin, as previously described (30).

In vivo glucose use index in individual tissues

To determine an index for the glucose use rate by individual tissues, a rapid iv injection of 20 μCi per mouse of D-(^{3}H)-2-deoxyglucose [D-(^{3}H)-2DG; PerkinElmer] was performed through the femoral vein 60 min before the end of the infusion period (30, 31). Plasma D-(^{3}H)-2DG disappearance and glucose concentration were determined in 5-μl drops of blood sampled from the tip of the tail vein at 0, 5, 10, 15, 20, 25, 30, 45, and 60 min after the injection. Diaphragm, heart, tibialis, vastus lateralis, and white adipose tissues were dissected out and immediately dissolved in NaOH to extract the D-(^{3}H)-2DG6-phosphate.

Isotope measurements

For glucose turnover measurements, the enrichments by D-(^{3}H-3)-glucose were determined from total blood after deproteinization by a $Zn(OH)_2$ precipitation as previously described (30, 31). Briefly, an aliquot of the protein-free supernatant was evaporated to dryness and mixed with scintillation fluid to determine the radioactivity corresponding to D-(^{3}H-3)-glucose. In a second aliquot of the same supernatant, glucose concentration was measured by the glucose oxidase method (Trinder, Sigma).

For individual tissue glucose use measurements, plasma D-(^{3}H)-2DG was determined from total blood after deproteinization with a $Zn(OH)_2$ precipitation, and tissue D-(^{3}H)-2DG and D-(^{3}H)-2DG-6 phosphate contents were determined as previously described (30, 31). Briefly, a piece of each tissue was dissolved in 1 M NaOH at 55 C for 60–120 min and then neutralized with 1 M hydrochloric acid. D-(^{3}H)-2DG 6-phosphate and D-(^{3}H)-2DG were differentially precipitated by the use of a zinc hydroxide (0.3 M) or a perchloric acid solution (6%) (27).

Body composition

Gonadal fat pads were carefully dissected out and weighed. The whole carcasses were chopped and dried to a constant weight at 70 C in potassium hydroxide (1 M) and then subsequently homogenized. Total body fat content was determined by the Soxhlet extraction method using petroleum benzine.

Histological analysis of gonadal fat pads and determination of adipocyte size and DNA content

Gonadal adipose tissue was removed from each animal and fixed in 10% formaldehyde/PBS and maintained at 4 C until used in a sucrose solution. Fixed specimens were embedded in tissue-freezing medium and frozen in isopentane cooled with liquid nitrogen. The tissue was cut into 14-μm sections that were mounted on slides and was stained with hematoxylin and eosin or with oil red O. The DNA content of adipose tissue was measured as an index of adipocyte number. Frozen gonadal adipose tissue was incubated overnight in the presence of Proteinase K (250 μg). Genomic DNA was purified using phenol/chloroform and then quantified by measuring the absorbance at 260 nm.

Western blot analysis

White adipose tissue was harvested in a HEPES (25 mM)-sucrose (250 mM)-EDTA (2 mM) buffer at a 1:6 weight to volume ratio. Thirty micrograms of whole protein extract were separated by electrophoresis on a 12% sodium dodecyl sulfate-polyacrylamide gel and transferred onto a polyvinyl difluoride membrane. Red Ponceau staining was performed to ensure of an equal loading of each lane. GLUT4 was then immunodetected with a specific primary antibody (Santa Cruz Biotechnology, La Jolla, CA) and a secondary antibody linked to horseradish peroxidase (DakoCytomation, Glostrup, Denmark) and revealed by chemiluminescence. Band analyses were performed by scanning the corresponding autoradiograph. The densitometric values were obtained and quantified using the Image Quant software (Amersham Bioscience, Lyon, France).

PPARα recombinant adenovirus

Briefly, after mutation of the *Pac*I site in the 3′ noncoding region, the cDNA of the murine PPARα gene was subcloned into the pAdTrack-cytomegalovirus shuttle vector coexpressing green fluorescent protein (GFP). The corresponding recombinant adenoviral vector was obtained as previously described (32). Adenovirus expressing only GFP was used as a control (Genethon, Nantes, France). PPARα adenoviruses were propagated in AD-293 cells and purified by cesium chloride density centrifugation.

Adenovirus infection

In mice bearing an intrafemoral catheter, 5.5×10^8 pfu of an adenovirus expressing the GFP and PPARα were injected in a total volume of 100 μl. Six days later basal glucose turnover was assessed. At the end of the experiment, the livers were removed and fixed with a formaldehyde buffer [PBS 0.1 M (pH 7.4), 4% picric acid, and 4% formaldehyde], cryoprotected 1 night in 20% sucrose, and observed by UV to quantify approximately the percentage of cells of infected by the adenovirus.

RT-PCR analyses

Reexpression of PPARα in the liver was evaluated by quantitative RT-PCR analysis. Briefly, the total RNA (500 ng) was reverse transcribed for 1 h at 42 C in a 20-μl final volume reaction mixture containing 50 mM Tris-HCl, 75 mM KCl, 3 mM $MgCl_2$, 10 mM dithiothreitol, 250 mM random hexamers (Promega, Charbonnieres, France), 250 ng oligo(dT) (Promega), 2 mM of each deoxynucleotide triphosphate, and 100 U Superscript II reverse transcriptase (Invitrogen, Carlsbad, CA). Real-time quantitative PCR analysis was performed starting with 6.25 ng of reverse-transcribed total RNA in a final volume of 10 μl PCR, with 0.5 μM of each primer (Invitrogen), 2 mM $MgCl_2$, using 1 × LightCycler DNA Master SYBR Green I mix in a light cycler instrument (Roche Molecular Biochemicals, Mannheim, Germany). Samples were incubated in the LightCycler apparatus for an initial denaturation at 95 C for 10 min, followed by 40 cycles. Each cycle consisted of 95 C for 15 sec, 58 C for 7 sec, and 72 C for 15 sec. The primers used to detect PPARα were 5′-CGGCCTGGCCTTCTAAACA-3′ for sense and 5′-TTTGGGAA-GAGGGTGTCA-3′ for antisense oligonucleotides.

RT-PCR analyses were similarly performed to assess the concentration of hexokinase II (HKII), fatty acid synthase (FAS), and acetyl-coenzyme A carboxylase (ACC) in white adipose depots. Total RNA from adipose tissue samples was prepared using the RNeasy kit (QIAGEN, Courtaboeuf, France). The absolute concentrations of FAS, HKII, and ACC mRNAs were determined by reverse transcription (RT) followed by real-time PCR using a Light-Cycler (Roche Diagnostics). First-strand cDNAs were first synthesized from 1 μg of total RNA in the presence of 100 U of Superscript II (Invitrogen, Cergy-Pontoise, France) using both random hexamers and oligo (dT) primers (Promega). The real-time PCR was performed in a final volume of 20 μl containing 5 μl of a 60-fold dilution of the RT reaction medium, 15 μl of reaction buffer from the FastStart DNA Master SYBR Green kit (Roche Diagnostics), and 10.5 pmol of the specific forward and reverse primers (Eurobio, Les Ulis, France). The list of the primers is: HKII forward, CAA-GCG-TGG-ACT-GCT-CTT-CC; HKII reverse, TGT-TGC-AGG-ATG-GCT-CGG-AC; FAS forward, GTG-CAC-CCC-ATT-GAA-GGT-TCC; FAS reverse, GGT-TTG-GAA-TGC-TGT-CCA-GGG; ACC1 forward, GAG-CAA-GGG-ATA-AGT-TTG-AG; and ACC1 reverse, AGG-TGC-ATC-TTG-TGA-TTA-GC. For quantification, a standard curve was systematically generated with six different amounts (150 to 30,000 molecules/tube) of purified target cDNA cloned in the pGEM plasmid (Promega). Each assay was performed in duplicate, and validation of the real-time PCR runs was assessed by evaluation of the melting temperature of the products and the slope and error obtained with the standard curve. The analyses were performed using the LightCycler software (Roche Diagnostics). The results were presented as relative mRNA levels. Each absolute value of the mRNA of the genes of interest was compared with hypoxanthine guanine phosphoribosyltransferase expression in the same RT samples.

Nutritional regulation of hypothalamic gene expression, RNA isolation, and RT-PCR analysis

The concentration of mRNA of NPY, agouti-related protein (AgRP), POMC, and CART in the hypothalamus was determined in control and PPARα$^{-/-}$ mice during fasted and fed states (n = 5–7). Total RNA was isolated from the hypothalami with TriPure isolation reagent (Roche), and single-strand cDNA was synthesized from 1 μg of total RNA by using oligo dT (RT kit; Promega). Quantitative PCR was carried out with first-strand cDNA using the following primers for the hypothalamic peptides: NPY sense, 5′-CAGAAAACGCCCCCAGAAC-3′, antisense, 5′-CGGGAGAA-CAAGTTTCATTTCC-3′; AgRP sense, 5′-CGGAGGTGCTAGATCCA-CAGA-3′, antisense, 5′-AGGACTCGTGCAGCCTTACAC-3′; POMC sense, 5′-AGGCCTGACACGTGGAAGAT-3′, antisense, 5′-AGCAG-GAGGGCCAGCAA-3′; CART sense, 5′-TTCCTGCAATTCTTTCCTCT-TGA-3′, antisense, 5′-GGGAATATGGGAACCGAAGGT-3′; and as internal control RPL-19 sense 5′-GAAGGTCAAAGGGAATGTGTTCA-3′, antisense 5′-CCTTGTCTGCCTTCAGCTTGT-3′ on an ABI Prism 5700HT sequence detection system, with SYBR green reagents (Applied Biosystems

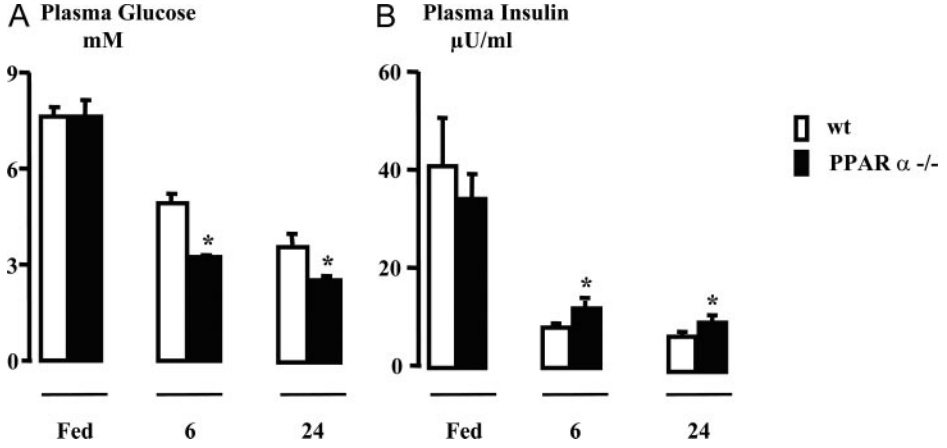

FIG. 1. Fasting-induced hypoglycemia in PPARα-null mice. Blood glucose (millimoles) (A) and plasma insulin (microunits per milliliter) (B) in control (*open bars*, wild type) and PPARα-null (*closed bars*, PPARα$^{-/-}$) mice in the fed state and after 6 and 24 h of fasting. The number of analyses ranges between six and 12 mice per group. *, Statistically different from control mice when $P < 0.05$.

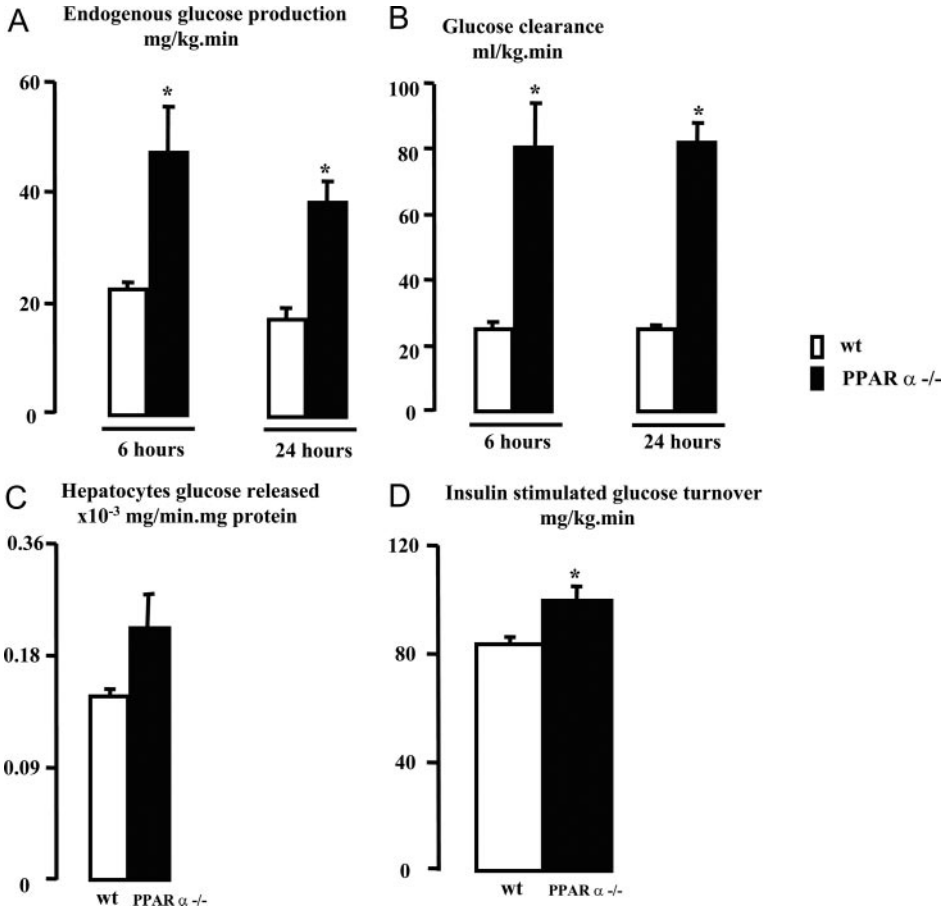

FIG. 2. EGP production and glucose clearance rates are elevated, whereas hepatocyte glucose production rate is normal in PPARα-null mice. EGP (milligrams per kilogram per minute) (A) and glucose clearance rates (milliliters per kilogram per minute) (B) were assessed in 6 and 24 h fasted controls [*open bars*, wild type (wt)] and PPARα-null mice (*closed bars*, PPARα$^{-/-}$). The EGP rate was elevated in PPARα-null mice and was associated with an increase in the rate of whole-body glucose clearance. The number of analysis ranged between five and seven mice per group. *, Statistically different from control mice when $P < 0.05$. C, The glucose release rate (10^{-3} mg/min·mg protein) was assessed in isolated hepatocytes. Glucose release was not different between both groups. The analysis was carried out with hepatocytes isolated from three mice in each group. D, Whole body glucose turnover stimulated by insulin (milliliters per kilogram per minute) was increased in PPARα$^{-/-}$ mice during euglycemic hyperinsulinemic clamp. The number of analysis ranged from five to seven mice per group. *, Statistically different from control mice when $P < 0.05$.

Inc., Foster City, CA) in duplicate, and the data were analyzed according to the $2^{-\Delta\Delta CT}$ method. The identity and purity of the amplified products was checked by analyzing the melting curve carried out at the end of amplification. To ensure the quality of the measurements, each plate included a negative control for each gene.

Intracerebroventricular infusion of WY14643

Chronic treatment. On d 1, the animal was anesthetized and a 1-cm midline incision was made in the skin over the skull. The animal was then placed on a stereotaxic apparatus and the periosteum cleaned as previous described (30). A hole, 1 mm in diameter, was made 0.1 mm laterally and 0.22 mm anteroposterior from the bregma, and a cannula (Alzet, Lupertino, CA) was inserted to a depth of 1.7 mm. Two supporting screws were placed bilaterally, one in the posterior quadrants and the other one in the anterior part of the skull, and secured in place with acrylic dental cement (Magasin Général Dentaire, Paris, France). The cannula was filled with artificial cerebral fluid (Harvard Apparatus, Les Ulis, France) and connected to a sealed Tygon catheter. On d 7, mice were implanted with an intrafemoral catheter. On d 14, WY14643 [4-chloro-6-(2,3-xilidino)-2-pyrimidinylthio acetic acid; Calbiochem, San Diego, CA], a specific PPARα activating ligand (33) used in rodents or the vehicle [dimethyl sulfoxide (DMSO); Sigma Aldrich, St quentin Fallavier, France; 50% in NaCl 0.9%] were infused continuously at a rate of 0.5 μl/h (1 mg/kg·d) using an osmotic minipump implanted sc and connected to the intracerebroventricular catheter. On d 21 glucose turnover was analyzed.

Acute treatment

The first steps of the acute treatment were similar from d 1 to 14 of the chronic procedure. On d 14, after 6 h of fasting, WY14643 or DMSO-NaCl 0.09% was infused into the lateral ventricle of the brain over 3 h at a rate similar to the chronic procedure.

Calculations

Calculations for glucose turnover measurements were made from parameters obtained during the last 60 min of the infusions in steady-state condition as previously described (20, 24). Briefly, the specific activity of the D-(^{3}H)3-glucose was calculated by dividing the D-(^{3}H)3-glucose enrichment by the plasma glucose concentration. The whole-body glucose turnover rate was calculated by dividing the rate of D-(^{3}H)3-glucose infusion by the D-(^{3}H)3-glucose-specific activity in the plasma. Whole-body glucose clearance rates were calculated by dividing the glucose turnover rate by the level of glycemia. For each mouse the mean values have been calculated and averaged with values from mice of the same group. Mice showing variations of the steady-state D-(^{3}H)3-glucose-specific activity greater than 15% during this time period were excluded from the study.

Statistical analysis

Results are presented as means ± SE. Statistical significance of differences was analyzed by using Student's *t* test for unpaired bilaterally distributed values of unequal variance. Two values were considered different from each other when $P < 0.05$.

Results

Blood parameters

In the fed state, blood glucose concentrations were similar in both control and PPARα-null mice (Fig. 1A). However, during fasting, glycemia decreased in both groups, although this reduction was more pronounced in the PPARα-null mice at both 6 and 24 h of fasting. Conversely, whereas plasma insulin concentrations were similar between groups in the

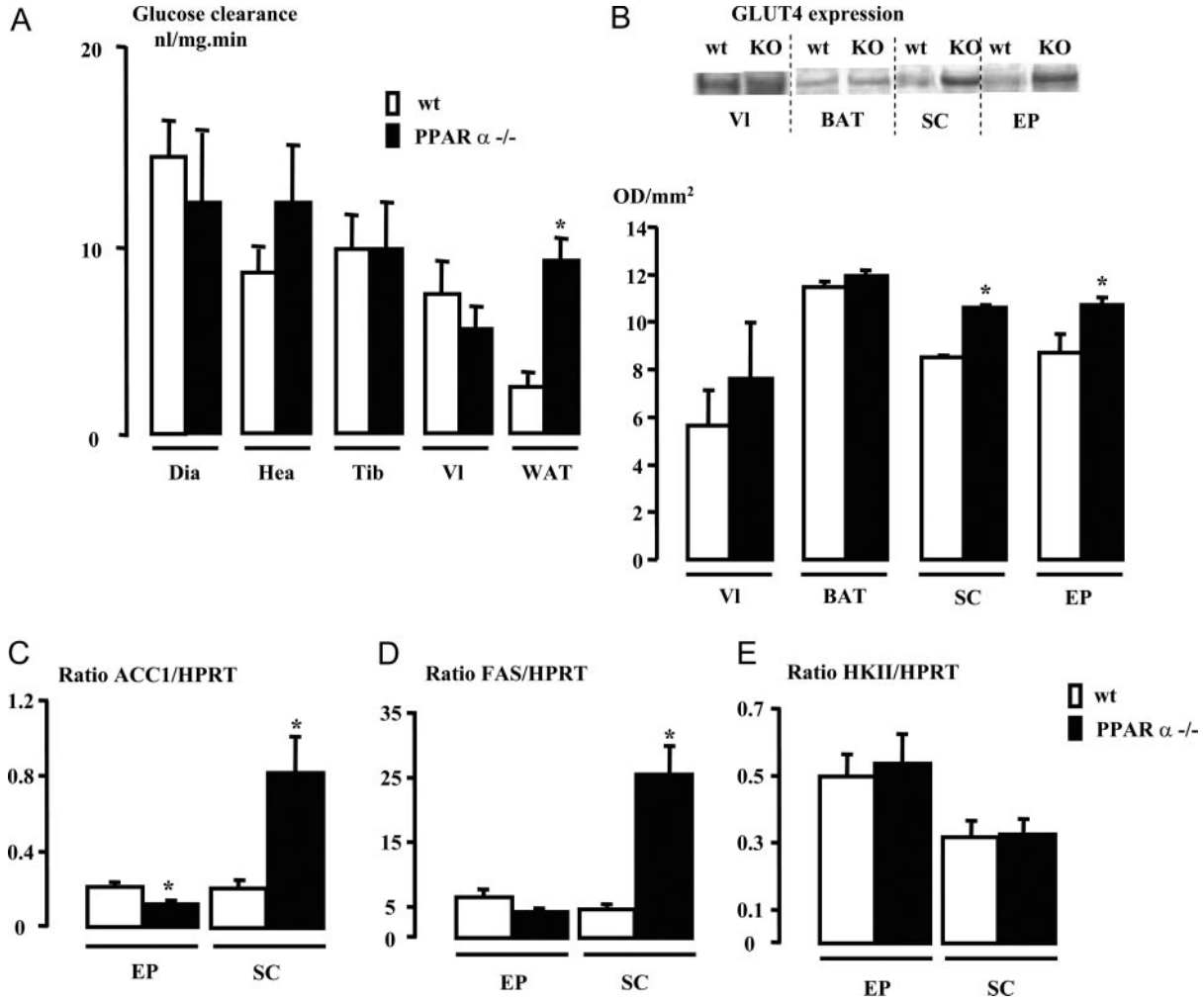

FIG. 3. White adipose tissue glucose clearance is increased in PPARα$^{-/-}$ mice. A, Individual tissue glucose clearance (nanoliters per milligram per minute) was assessed in diaphragm (Dia), heart (Hea), tibialis anterior (Tib), vastus lateralis (Vl), and perigonadal white adipose tissue (WAT). B, Representative Western blot analysis and quantification of GLUT4 content in vastus lateralis (Vl), brown adipose (BAT), sc (SC), and epididymal (EP) adipose depots after 24 h of fasting. Data are expressed as mean OD (square millimeters ± SE). Two representative samples per group are shown from a cohort of five to six per group. Red Ponceau staining was performed to ensure similar loading between lanes. The ratio of the mRNA content between hypoxanthine guanine phosphoribosyltransferase (HPRT) and ACC (C), FAS (D), and HKII (E) in EP and sc adipose depots. *, Statistically different from control mice when $P < 0.05$. OD (square millimeters) represents densitometric arbitrary units. Six mice per group were studied. KO, Knockout.

fed state, in the fasted state, they were higher in the PPARα-null mice than the control wild type (Fig. 1B).

In vivo and in vitro glucose fluxes

To determine whether the hypoglycemia of PPARα null mice was due to reduced endogenous glucose production, we quantified the endogenous glucose production rate (EGP) after 6 and 24 h of fasting. EGP was increased in all instances in the PPARα-null mice over the value of the control mice (Fig. 2A). Because the blood glucose levels were different between the controls and the PPARα-null mice in the fasted state, we calculated the blood glucose clearance rates. They were also higher in the PPARα-null than control mice, showing that the hypoglycemia could not be caused by a reduced EGP because EGP was actually increased but was associated more with increased glucose use (Fig. 2B). This conclusion was further confirmed by the assessment of glucose production by isolated hepatocytes incubated in the presence of pyruvate and lactate as gluconeogenic precursors. Glucose production was not statistically different in fasted control and PPARα-null hepatocytes (Fig. 2C). To assess whether the increased whole-body glucose clearance rate could be associated with increased insulin sensitivity, we assessed insulin action *in vivo* by the euglycemic hyperinsulinemic clamp technique. Whole-body insulin sensitivity was increased by 15% in the PPARα-null mice when compared with control mice (Fig. 2D).

Individual tissue glucose clearance and gene expression in the fasting state

To determine which tissue was responsible for the increased whole-body glucose use in the fasted state, we assessed the glucose clearance rates of individual tissues (Fig. 3A). The glucose clearance rate was increased 5-fold in go-

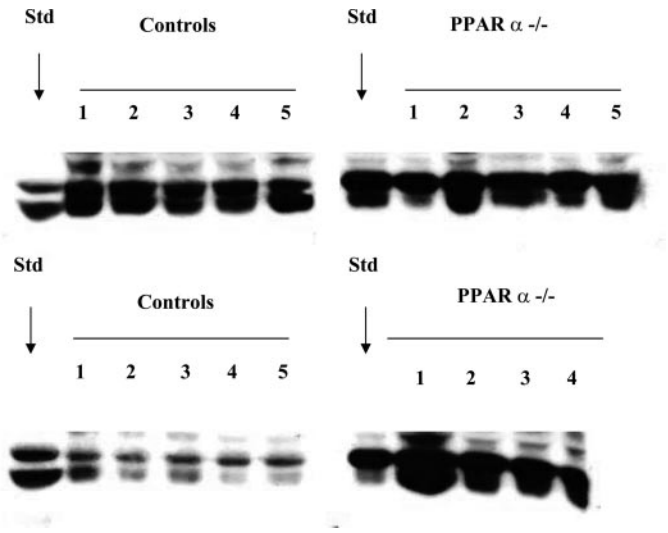

FIG. 4. Adipose tissue GLUT4 concentration is not reduced during fasting in PPARα$^{-/-}$ mice. Representative Western blot analyses of GLUT4 content in perigonadal adipose tissue after 24 h of fasting. The *upper row* corresponds to the fed condition and the *lower row* to the fasted condition. The *left lane* of each blot corresponds to an internal standard (Std). Lanes 1–5 correspond to different mice for each condition, excepted for fasted PPARα knockout mice in which only four animals have been studied. Red Ponceau staining was performed to ensure similar loading between lanes.

nadal white adipose tissue of PPARα-null mice, compared with the controls, whereas it was not significantly different between other tissues of control and PPARα-null mice.

To determine whether the increased glucose clearance by adipose tissue could be due to an up-regulation of GLUT4 expression, we evaluated the concentration of this transporter by Western blot analysis in the fasted state. Figure 3B shows that GLUT4 concentration was similar in muscle and brown adipose tissue of both control and mutant mice. Conversely, it was increased by 25 and 23% over controls in sc and epididymal adipose depots, respectively. Importantly, in the knockout mice, sc adipose tissue, ACC mRNA (Fig. 3C) and FAS mRNA (Fig. 3D) concentrations were increased, whereas HKII mRNA was unchanged (Fig. 3E). Conversely, in the epididymal adipose depot, a small but significant decrease in ACC mRNA (Fig. 3C) was observed. We then studied whether GLUT4 overexpression in adipose tissue was regulated by the fed-to-fasted transition. Whereas the fed-to-fasted transition was associated with a 90% reduction in GLUT4 concentration in adipocytes from control mice, in the PPARα-null mice, the level of GLUT4 was not reduced (Fig. 4).

Body weight, composition, and adipocyte studies

Body weight, gonadal pad weight, and total lipid content were 15, 40, and 20% higher in PPARα-null than age matched control mice, respectively (Fig. 5, A–C), whereas the lean mass was not significantly different (Fig. 5D). The total DNA content of gonadal fat pads per gram of body weight was increased by 30% in PPARα-null mice (Fig. 6A), but the DNA content per gram of gonadal tissue was reduced by 37%, indicating therefore an increase in adipocyte size (Fig. 6B). This was confirmed by histological analysis of sections from gonadal fat pads, which showed white adipocytes with larger cell diameters (Fig. 6C).

Reexpression of PPARα in the livers of knockout mice did not rescue the metabolic phenotype

A PPARα-mediated expression adenovirus was used to reexpress the gene in the liver of mutant mice (Fig. 7A). More than 90% of the hepatocytes reexpressed the gene (Fig. 7B). Six days after reexpression of PPARα, the glucose turnover rate was not different from the controls infected with a GFP-expressing adenovirus (Fig. 7C). No other tissue was infected by adenovirus treatment (Fig. 7D). Body weight, postprandial glycemia, and insulinemia were followed over 6 d after adenovirus injection and remained unchanged (not shown).

Effect of WY14643 infusion into the brain

PPARα is expressed in the brain, which is a major organ involved in the control of glucose homeostasis (9). To analyze the role of PPARα in the brain on the control of glucose homeostasis, we infused WY14643 into the brain using either osmotic minipumps for 7 d or an indwelling catheter for 3 h.

In the chronically treated mice, the whole-body glucose turnover and glycolytic and glycogen synthesis rates were reduced by 50–70% (Fig. 8). Similar results were observed in acutely treated mice (Fig. 9). Furthermore, WY14643 had no effect on glucose use in PPARα mutant mice, and no effects on body weight, glycemia, and insulinemia were detected (not shown).

To further delineate the role of PPARα in the brain for the control of glucose use by the different tissues, we quantified 2-deoxyglucose use in wild-type mice infused with WY14643 into the brain for 3 h. The data show that 2-deoxyglucose use was reduced in adipose depots, reaching significance in the epididymal fat pad (Fig. 10A). Conversely, no difference was noted in all the muscles studied (Fig. 10A) and brown adipose tissue (Fig. 10B).

Neuropeptide mRNA concentrations in the hypothalamus of wild-type and PPARα$^{-/-}$ mice in fast and fed states

To provide support for a role of PPARα in the brain as a regulator of glucose homeostasis, we performed RT-PCR analyses to quantify the concentration of 2-orexigenic (NPY, AgRP) and 2-anorexigenic neuropeptides (POMC, CART) mRNAs in the hypothalamus in fed and fast conditions. In the wild-type mice, the fed-to-fasting transition was accompanied by a significant increase in NPY and AgRP mRNAs and decrease in POMC and CART mRNA concentrations in

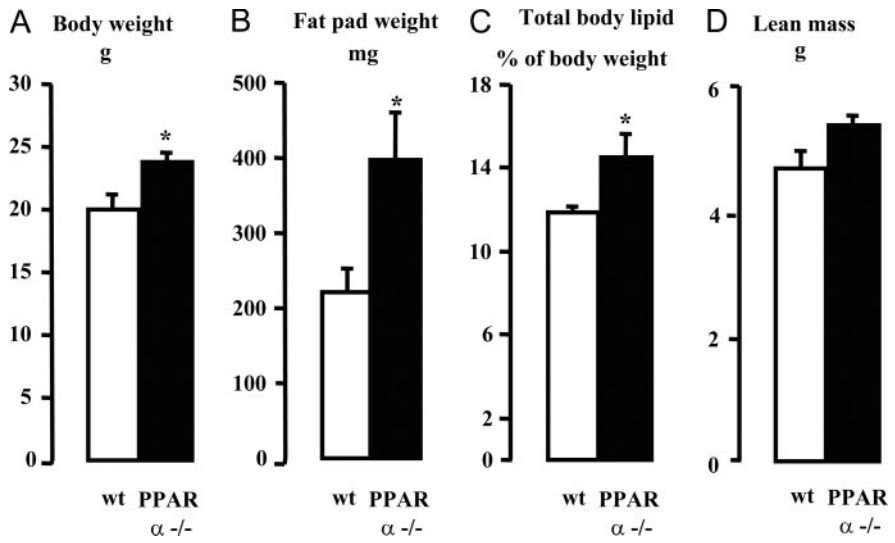

FIG. 5. Increased fat mass in PPARα$^{-/-}$ mice. Body weight (grams) (A), fat pad weight (milligrams) (B), total body lipid (percent of body weight) (C), and lean mass (grams) (D) of controls [wild type (wt), *open bars*] and PPARα$^{-/-}$ mice (*closed bars*). The number of analyses is seven mice per group. *, Statistically different from control mice when $P < 0.05$.

the hypothalamus (Fig. 11, A–D). Conversely, in the mutant mice, the mRNA concentrations of AgRP and POMC were the only ones to follow those of the wild-type mice (Fig. 11, A–D). Importantly, the fed mRNA concentrations of NPY and POMC were higher in the mutant than the wild-type mice, whereas in the fasting state, no significant differences were noted between the two groups of mice.

Discussion

The lack of PPARα in mice induces a dramatic hypoglycemia during fasting. Here we show that in the absence of this transcription factor, whole-body glucose use, white adipose tissue glucose use, GLUT4 expression, fat mass, and insulin sensitivity are all increased. The lack of PPARα in the liver was not involved in this phenotype because adenovirus-mediated PPARα reexpression in the liver did not revert the phenotype to normal. Conversely, when a PPARα agonist was infused into the brain of a wild-type mouse, whole-body and adipose tissue glucose use was reduced. Our data suggest that central nervous PPARα has an important role in the control of whole-body glucose homeostasis.

In a first set of experiments, we assessed fasted and fed plasma parameters and confirmed that in the PPARα-null mice, blood glucose levels decreased rapidly after food removal and remained in the hypoglycemic range (34). This was associated with hyperinsulinemia as previously described when the mice were fed a normal chow (16) or a high-fat diet (35). These confirmatory results further demonstrate that glucose homeostasis is impaired in the absence of PPARα. Several organs have key functions in the regulation of glycemia, with the liver producing glucose during the fasting state to supply other organs. We show here that hepatic glucose production, although increased over controls, was ineffective in maintaining normal glycemia during long-term fasting, *i.e.* when gluconeogenesis is fully active. This mechanism could be related either to an impaired glucose futile cycling (36), resulting in a lower capacity to produce glucose by gluconeogenesis, or to excessive peripheral

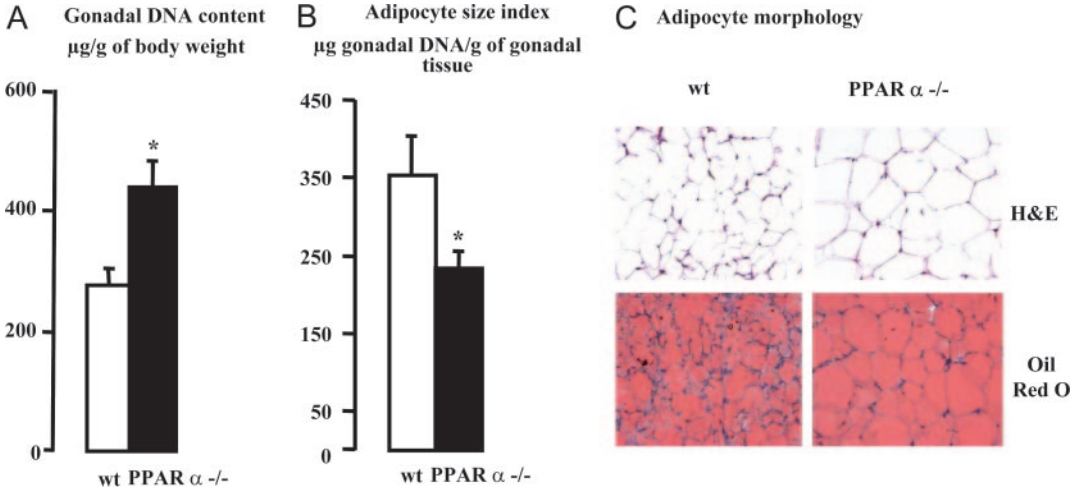

FIG. 6. PPARα$^{-/-}$ mice fat pads have more adipocytes and are of larger size. A, Gonadal fat DNA content (micrograms per gram of body weight) of controls [wild type (wt), *open bars*] and PPARα$^{-/-}$ mice (*closed bars*). B, Adipocyte size index (micrograms of gonadal DNA per gram of gonadal tissue). C, Adipocyte morphology. Hematoxylin and eosin (H&E) or oil red O staining. *, Statistically different from control mice when $P < 0.05$.

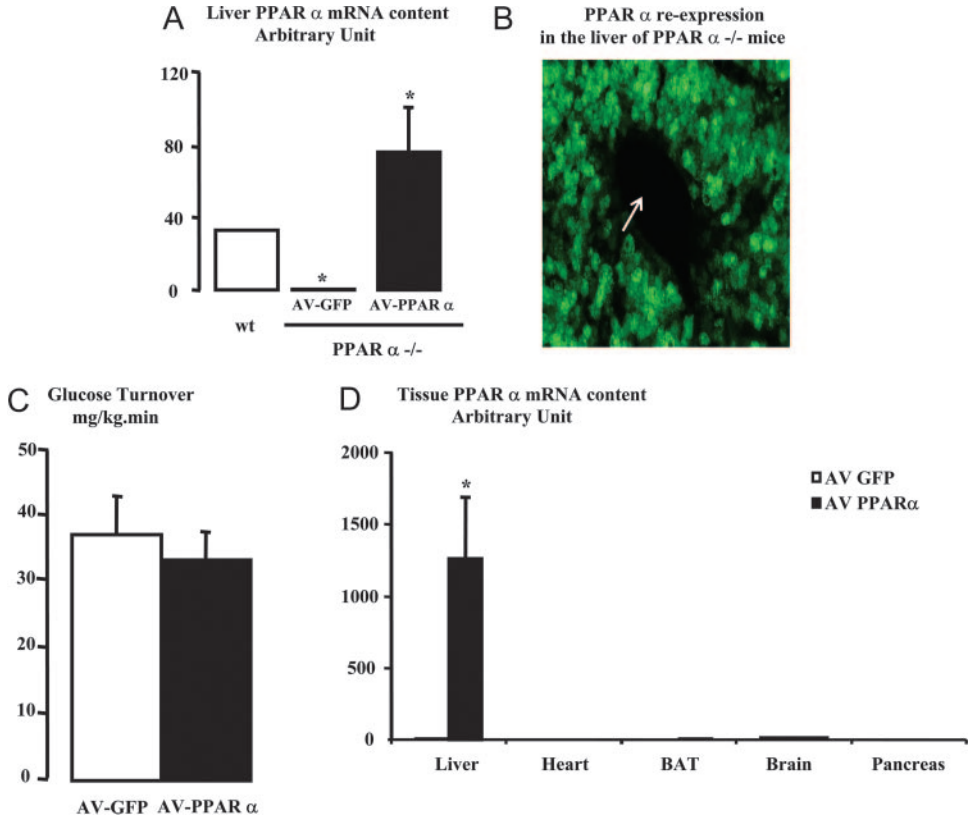

FIG. 7. Reexpression of PPARα in liver of knockout mice does not rescue the metabolic phenotype. A, Relative PPARα mRNA content in the liver of wild-type [wild type (wt), *open bars*] and PPARα-null mice infected with GFP (AV-GFP) or PPARα (AV-PPARα) expressing adenovirus (*closed bars*). B, Histological representation of a liver slice showing that more than 90% of the hepatocytes were reexpressing the gene in PPARα$^{-/-}$ mouse expressing AV-PPARα. *White arrow* shows a centrolobular vein. C, Basal glucose turnover (milligrams per kilogram per minute) in PPARα$^{-/-}$ mice infected with AV-GFP (*open bars*) or AV-PPARα (*closed bars*). No difference was noted between groups. D, Relative PPARα mRNA content (arbitrary units) in different tissues of PPARα$^{-/-}$ mice infected with AV-GFP (*open bars*) or AV-PPARα (*closed bars*). The number of analyses was six mice per group.*, Statistically different from AV-GFP-infected mice or wt when $P < 0.05$.

glucose use. Whereas the former hypothesis has previously been validated, we further assessed whether the second hypothesis was also relevant. We found that whole-body glucose use was dramatically increased during fasting in the PPARα-null mice. This was associated with an excessive glucose use rate and a high GLUT4 content in perigonadal and sc adipose depots. The increased GLUT4 was not observed in either interscapular brown fat or muscles. Importantly, the fed-to-fasted transition did not affect the perigonadal GLUT4 content in the knockout mouse, showing the strong impact of the lack of PPARα on the regulation of GLUT4 expression. Interestingly, the increased adipose tissue GLUT4 content was associated with an increased FAS and ACC mRNA but not HKII mRNA concentration in sc adipose depots. However, no changes or a slight decrease of the concentration of these mRNAs was detected in the epididymal adipose depot. An increased GLUT4 in adipose tissue is sufficient in itself to increase glucose use and fat accumulation (37). Furthermore, we show that whole-body insulin sensitivity was increased by 15%, which could be due solely to the increased adipose tissue GLUT4. This hypothesis has been proposed previously in mice overexpressing GLUT4 in white adipose tissue. Such mice were resistant to streptozotocin-induced diabetes (38).

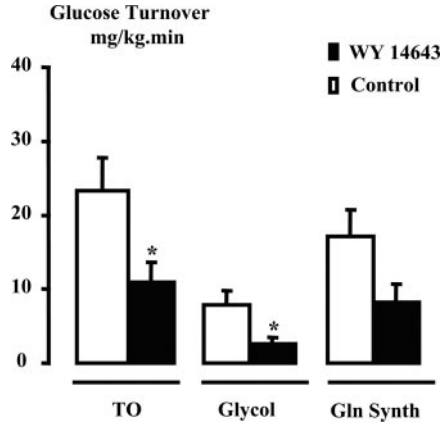

FIG. 8. A chronic infusion of a PPARα agonist into the brain reduces whole-body glucose turnover and glycolysis but not glycogen synthesis. Basal whole-body glucose turnover (TO), glycolysis (Glycol), and glycogen synthesis (Gln Synth) rates (milligrams per kilogram per minute) were assessed after a 7-d chronic infusion of PPARα agonist (WY14643, *closed bars*) or DMSO-NaCl 0.9% (controls, *open bars*) in mice. *, Statistically different from DMSO-infused mice when $P < 0.05$. Seven mice per group were studied.

An interesting question remaining is to understand why GLUT4 was overexpressed in white adipose depots only and not in brown adipose depot or muscles. Hyperinsulinemia is certainly a strong regulator of GLUT4 expression in adipose depots (39). A slight hyperinsulinemia is observed in PPARα$^{-/-}$ fasted mice and could contribute at least in part to the mechanism. However, insulin also increases GLUT4 expression in brown adipose tissue (40), but no changes have been observed in PPARα$^{-/-}$ mice. Therefore, other mechanisms could be implicated, including numerous factors linked to adipocyte differentiation or energy metabolism. The differentiation and maintenance of adipose tissue is driven by the transcription factor PPARγ, a member of the nuclear receptor family (41). PPARγ heterodimerizes with retinoid X receptor-α and controls transcription of target genes by binding to a direct repeat-1 PPARγ response ele-

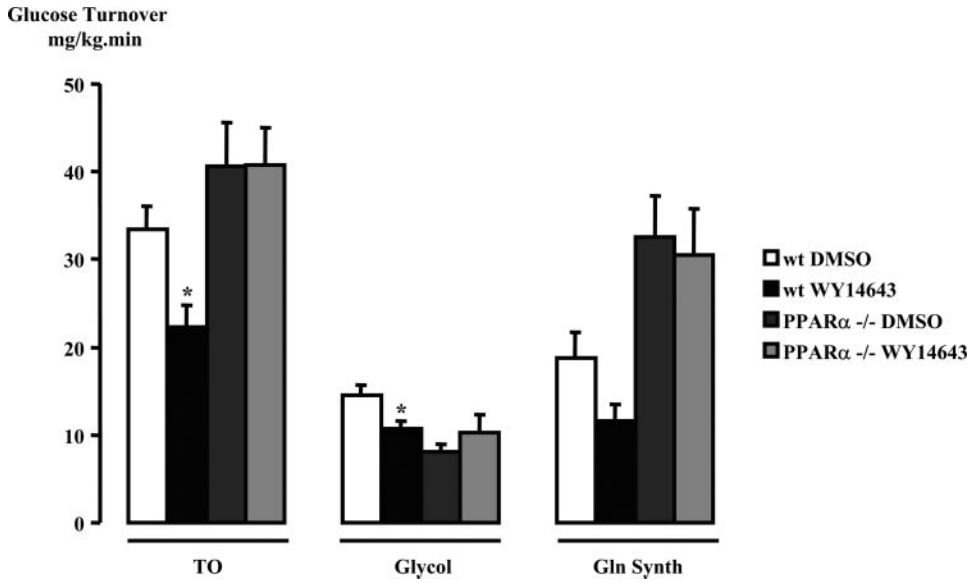

FIG. 9. An acute 3-h infusion of a PPARα agonist into the brain reduces whole-body glucose turnover. Basal whole-body glucose turnover (TO), glycolysis (Glycol), and glycogen synthesis (Gln Synth) rates (milligrams per kilogram per minute) were assessed after a 3-h PPARα agonist (WY14643, *closed bars*) or DMSO-NaCl 0.9% (controls, *open bars*) infusion in wild-type (wt) and PPARα knockout (PPARα$^{-/-}$) mice. *, Statistically different from DMSO-infused mice when $P < 0.05$. Seven mice per group were studied.

ment located in the promoter of target genes (42). Similarly, it has been shown that liver X receptors, expressed in adipose tissues, are involved in the regulation of adipose tissue fatty acid metabolism, triglyceride storage, and in addition, they increase GLUT4 expression in adipocytes (43). Therefore, one could suggest that the elevated free fatty acid concentrations characteristic of the PPARα$^{-/-}$ mice (9) could contribute to the GLUT4 regulation. We also evaluated the consequences of adipose tissue GLUT4 overexpression on whole-body fat mass and showed that body weight, fat pad weight, adipocyte size, and the number of adipocytes were increased in the PPARα knockout mice. Because the corresponding transcription factor is not expressed, or only at trace levels, in adipose cells (44), we surmised that the regulation of whole-body glucose homeostasis would depend on the expression of PPARα in other cell types.

An important regulator of whole-body glucose homeostasis is the liver and PPARα is strongly expressed in hepatocytes. In a second set of experiments, we assessed whether the PPARα in the liver could be responsible for the phenotypes of the null mice. To achieve this, we reexpressed PPARα specifically in the liver by means of an adenovirus. In these mice, whole-body glucose use remained elevated, showing that PPARα in the liver was not responsible for the entire phenotype.

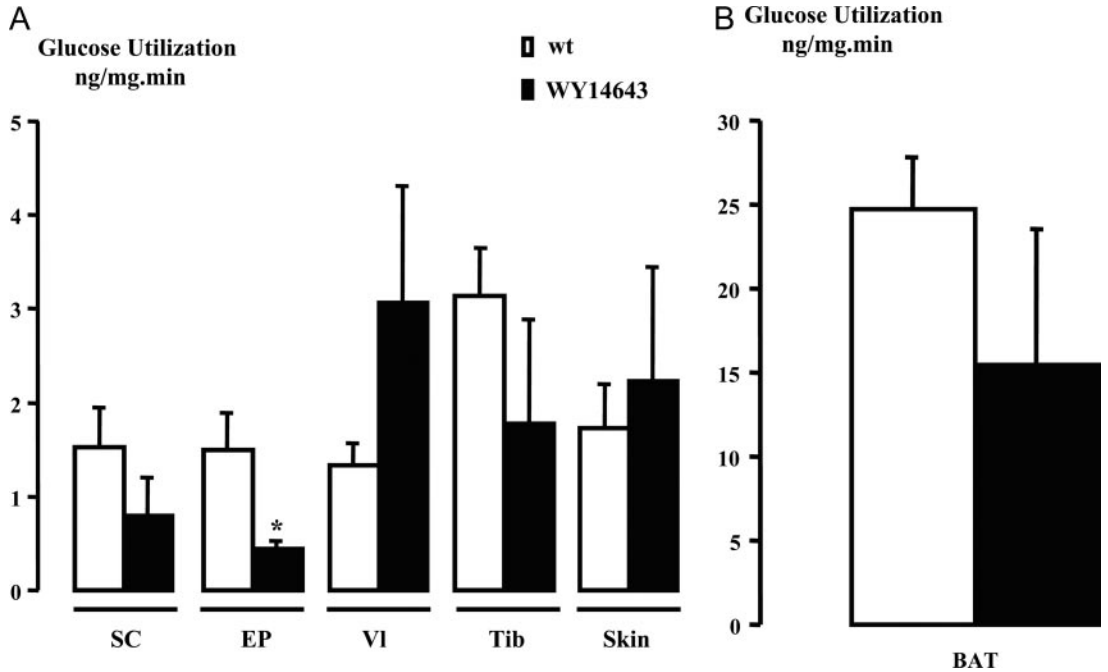

FIG. 10. An acute 3-h infusion of a PPARα agonist into the brain of wild-type (wt) mice controls adipose tissue glucose use. Individual tissue glucose use rate (nanograms per milligram per minute) was assessed during the basal state in sc (SC) and epididymal (EP) adipose depots, vastus lateralis (Vl), tibialis anterior (Tib), and skin (A) and in brown adipose tissue (BAT) (B). *, Statistically different from DMSO-infused mice when $P < 0.05$. Five mice per group were studied.

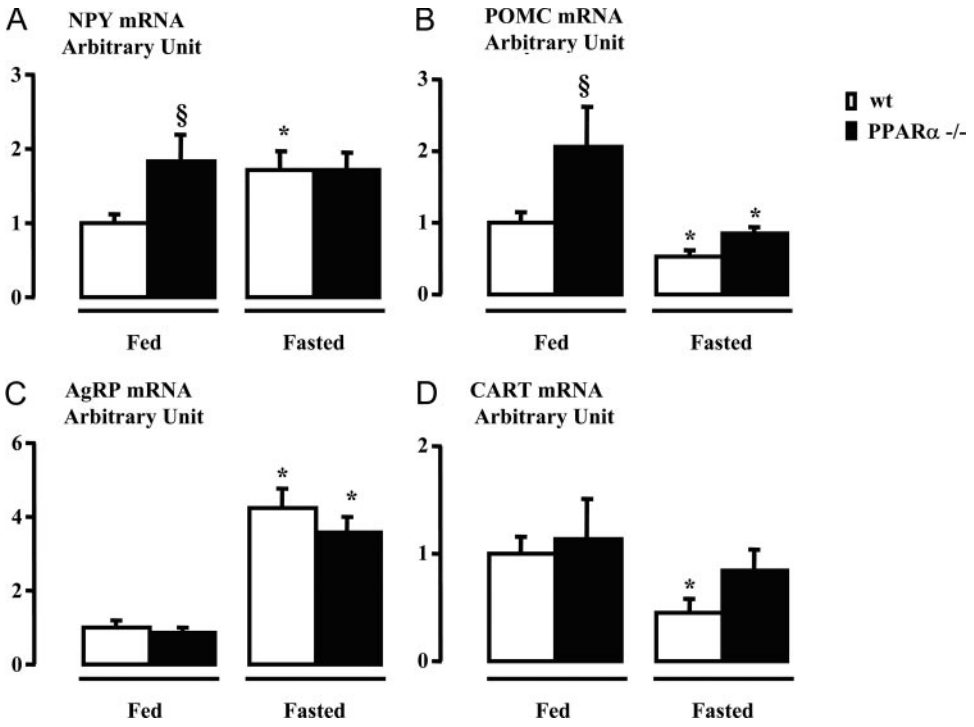

FIG. 11. Hypothalamic NPY, AgRP, POMC, and CART mRNA content during the fed-to-fasting transition. The hypothalamic mRNA content of the genes coding for NPY, AgRP, POMC, and CART was quantified in wild-type (wt, *open bars*) and PPAR$\alpha^{-/-}$ (*closed bars*) mice during the fed-to-fasting transition. *, Statistically different from wild-type mice when $P < 0.05$. §, Statistically different from the corresponding fed state when $P < 0.05$. Five to seven mice per group were studied.

Over recent years it has been demonstrated that the brain is a major regulator of whole-body glucose homeostasis. Because PPARα is expressed in the brain, we investigated whether the brain PPARα could be involved in the regulation of glucose metabolism. To do this, a third set of mice was infused for 7 d with the agonist WY14643 into the lateral ventricle of the brain. In these mice whole-body glucose use was dramatically reduced, suggesting that brain PPARα, when activated, reduces whole-body glucose use. We could not show a further reduction of white adipose tissue GLUT4 content because the latter is already dramatically reduced during fasting in normal mice (not shown). Interestingly, we performed similar experiments in which WY14643 was infused acutely for 3 h into the brains of wild-type and PPARα mutant mice. Adipose tissue glucose use and whole-body glucose turnover were reduced, therefore confirming the inhibitory effect of WY14643 on the control of whole-body glucose homeostasis. Importantly, this effect was specific because no differences were seen when WY14643 was infused into the brains of the PPARα-mutant mice.

The regulatory effect of PPARα in the brain could be related to its antiinflammatory effect (45). These authors showed that lipopolysaccharide-stimulated microglial cells have a reduced secretion of proinflammatory cytokines TNFα, IL-6, and reduced nitric oxide production in the presence of a WY14643 analog. Because inflammatory cytokines inhibit brain neuropeptides such as POMC (46), the regulatory role of cerebral neuropeptides on whole-body glucose homeostasis (46) could consequently be impaired in the absence of PPARα. The central regulation of whole-body glucose homeostasis is mediated by the autonomic nervous system (47). We and others have shown that nutrients and hormones can control whole-body glucose use and hepatic glucose production (27, 48–50). Therefore, through its regulatory effect on neuropeptides, PPARα could control whole-body glucose metabolism.

To challenge this hypothesis, we determined the mRNA concentration, in the hypothalamus, of orexigenic (NPY, AgRP) and anorexigenic (POMC, CART) peptides. Our data show that PPAR$\alpha^{-/-}$ mice exhibit an increased NPY mRNA concentration in the hypothalamus. This orexigenic neuropeptide has been shown to induce obesity when infused directly into the brain of rats (51). In that model the rats became hyperinsulinemic, which could, at least in part, be responsible for the increased energy storage. Hyperinsulinemia is a strong enhancer of GLUT4 gene expression in adipose tissue (39). Hence, it is possible that the slight hyperinsulinemia observed in the PPAR$\alpha^{-/-}$ mice could contribute to the increase in the GLUT4 content of adipose tissue. Whether the increase NPY mRNA concentration in the PPAR$\alpha^{-/-}$ mice is responsible for their hyperinsulinemia and the increased GLUT4 expression in adipose tissue remains to be determined. Furthermore, the mRNA content of POMC in the hypothalamus was also increased in PPAR$\alpha^{-/-}$ mice. POMC processing leads to the production of αMSH, a neuropeptide shown to increase insulin sensitivity (52). This feature matches the phenotype of the PPAR$\alpha^{-/-}$ mice, which are hypersensitive to insulin. Again it could be that in the absence of PPAR$\alpha^{-/-}$, the increased hypothalamic POMC concentration could be, at least in part, responsible for the increased sensitivity to insulin. This latter feature, associated with the excessive adipose tissue GLUT4 content, could certainly lead to increased energy storage and fasting-induced hypoglycemia as described for the PPAR$\alpha^{-/-}$ mice. AgRP and CART were also quantified. Whereas the concentration of CART was increased during fasting in PPAR$\alpha^{-/-}$ mice, its contribution to the phenotype remains unclear.

In conclusion, the lack of PPARα in null mice is associated, in the fasted state, with increased whole-body glucose use, white adipose tissue glucose use, and GLUT4 content, which could not be explained by the lack of PPARα in the liver. Conversely, our data suggest, albeit indirectly, that the absence of PPARα in the brain could contribute to the metabolic phenotype of the PPARα null mice.

Acknowledgments

We thank the vector team of the University Hospital of Nantes, supported by the Association Française contre les Myopathies, for amplifying the PPARα-GFP and GFP adenoviruses. The authors also thank Dr. A. Ait Belgnaoui for helpful criticisms.

Received December 5, 2005. Accepted June 5, 2006.

Address all correspondence and requests for reprints to: Rémy Burcelin, Unit Mixté de Recherche, 5018 Centre National de la Recherche Scientifique-University Paul Sabatier, IFR 31, Bt L1 Rue J. Poulhès, 31403 Toulouse, France. E-mail: burcelin@toulouse.inserm.fr.

This work was supported by grants from the Association de Langue Française pour l'Etude du Diabète et de Maladies Métaboliques (Roche Diagnostics-ALFEDIAM) and the Club d'Etude du Système Nerveux Autonome (to C.K.). R.B. is the recipient of an Action Thématique Incitative sur Theme-Centre National de la Recherche Scientifique program.

The authors declare that they have no conflict of interest with the presented data.

References

1. **Issemann I, Green S** 1990 Activation of a member of the steroid hormone superfamily by peroxisome proliferators. Nature 347:645–650
2. **Escher P, Wahli W** 2000 Peroxisome proliferator-activated receptors: insight into multiple cellular functions. Mutat Res 448:121–138
3. **Fruchart JC, Staels B, Duriez P** 2001 PPARs, metabolic disease and atherosclerosis. Pharmacol Res 44:345–352
4. **Kersten S, Desvergne B, Wahli W** 2000 Roles of PPARs in health and disease. Nature 405:421–424
5. **Hashimoto T, Cook W, Qi C, Yeldandi A, Reddy J, Rao M** 2000 Defect in peroxisome proliferator-activated receptor α-inducible fatty acid oxidation determines the severity of hepatic steatosis in response to fasting. J Biol Chem 275:28918–28982
6. **Minnich A, Tian N, Byan L, Bilder G** 2001 A potent PPARα agonist stimulates mitochondrial fatty acid β-oxidation in liver and skeletal muscle. Am J Physiol 280:E270–E279
7. **Schoonjans K, Staels B, Auwerx J** 1996 Role of the peroxisome proliferator-activated receptor (PPAR) in mediating the effect of fibrates and fatty acids on gene expression. J Lipid Res 37:907–925
8. **Aoyama T, Peters JM, Iritani N, Nakajima T, Furihata K, Hashimoto T, Gonzalez FJ** 1998 Altered constitutive expression of fatty acid-metabolizing enzymes in mice lacking the peroxisome proliferator-activated receptor α (PPARα). J Biol Chem 273:5678–5684
9. **Kersten S, Seydoux J, Peters J, Gonzalez F, Desvergne B, Wahli W** 1999 Peroxisome proliferator-activated receptor α mediates the adaptive response to fasting. J Clin Invest 103:1489–1498
10. **Patel D, Knight B, Wiggins D, Humphreys S, Gibbons G** 2001 Disturbances in the normal regulation of SREBP-sensitive genes in PPARα-deficient mice. J Lipid Res 42:328–337
11. **Chou CJ, Haluzik M, Gregory C, Dietz KR, Vinson C, Gavrilova O, Reitman ML** 2002 WY14,643, a peroxisome proliferator-activated receptor α (PPARα) agonist, improves hepatic and muscle steatosis and reverses insulin resistance in lipoatrophic A-ZIP/F-1 mice. J Biol Chem 277:24484–24489
12. **Boden G, Chen X, Ruiz J, White JV, Rossetti L** 1994 Mechanisms of fatty acid-induced inhibition of glucose uptake. J Clin Invest 93:2438–2446
13. **Boden G, Shulman GI** 2002 Free fatty acids in obesity and type 2 diabetes: defining their role in the development of insulin resistance and β-cell dysfunction. Eur J Clin Invest 32(Suppl 3):14–23
14. **Ye JM, Iglesias MA, Watson DG, Ellis B, Wood L, Jensen PB, Sorensen RV, Larsen PJ, Cooney GJ, Wassermann K, Kraegen EW** 2003 PPARα/γ ragaglitazar eliminates fatty liver and enhances insulin action in fat-fed rats in the absence of hepatomegaly. Am J Physiol Endocrinol Metab 284:E531–E540
15. **Ye JM, Doyle PJ, Iglesias MA, Watson DG, Cooney GJ, Kraegen EW** 2001 Peroxisome proliferator-activated receptor (PPAR)-α activation lowers muscle lipids and improves insulin sensitivity in high fat-fed rats: comparison with PPAR-γ activation. Diabetes 50:411–417
16. **Haluzik M, Gavrilova O, LeRoith D** 2004 Peroxisome proliferator-activated receptor-α deficiency does not alter insulin sensitivity in mice maintained on regular or high-fat diet: hyperinsulinemic-euglycemic clamp studies. Endocrinology 145:1662–1667
17. **Mavri A, Bastelica D, Staels B, El Ayachi S, Juhan-Vague I, Alessi MC** 2004 PPARα deficiency does not modify age dependency but prevents high fat diet increase in plasma PAI-1 as well as insulin resistance. Thromb Haemost 91: 1051–1052
18. **Guerre-Millo M, Rouault C, Poulain P, Andre J, Poitout V, Peters JM, Gonzalez FJ, Fruchart JC, Reach G, Staels B** 2001 PPARα-null mice are protected from high-fat diet-induced insulin resistance. Diabetes 50:2809–2814
19. **Kainu T, Wikstrom A, Gustafsson J, Pelto-Huikko M** 1994 Localization of the peroxisome proliferator-activated receptor in the brain. Neuroreport 5:2481–2485
20. **Cullingford TE, Dolphin CT, Sato H** 2002 The peroxisome proliferator-activated receptor α-selective activator ciprofibrate upregulates expression of genes encoding fatty acid oxidation and ketogenesis enzymes in rat brain. Neuropharmacology 42:724–730
21. **Cimini A, Cristiano L, Colafarina S, Benedetti E, Di Loreto S, Festuccia C, Amicarelli F, Canuto RA, Ceru MP** 2005 PPARγ-dependent effects of conjugated linoleic acid on the human glioblastoma cell line (ADF). Int J Cancer 117:923–933
22. **Garcia-Bueno B, Madrigal JL, Lizasoain I, Moro MA, Lorenzo P, Leza JC** 2005 Peroxisome proliferator-activated receptor γ activation decreases neuroinflammation in brain after stress in rats. Biol Psychiatry 57:885–894
23. **Lee JH, Joe EH, Jou I** 2005 PPAR-α activators suppress STAT1 inflammatory signaling in lipopolysaccharide-activated rat glia. Neuroreport 16:829–833
24. **Strakova N, Ehrmann J, Bartos J, Malikova J, Dolezel J, Kolar Z** 2005 Peroxisome proliferator-activated receptors (PPAR) agonists affect cell viability, apoptosis and expression of cell cycle related proteins in cell lines of glial brain tumors. Neoplasma 52:126–136
25. **Shimokawa T, Kumar MV, Lane MD** 2002 Effect of a fatty acid synthase inhibitor on food intake and expression of hypothalamic neuropeptides. Proc Natl Acad Sci USA 99:66–71
26. **Burcelin R, Crivelli V, Dacosta A, Roy-Tirelli A, Thorens B** 2002 Heterogeneous metabolic adaptation of C57BL/6J mice to high-fat diet. Am J Physiol Endocrinol Metab 282:E834–E842
27. **Perrin C, Knauf C, Burcelin R** 2004 Intracerebroventricular infusion of glucose, insulin, and the adenosine monophosphate-activated kinase activator, 5-aminoimidazole-4-carboxamide-1-β-D-ribofuranoside, controls muscle glycogen synthesis. Endocrinology 145:4025–4033
28. **Guillam M, Burcelin R, Thorens B** 1998 Normal hepatic glucose production in the absence of GLUT2 reveals an alternative pathway for glucose release from hepatocytes. Proc Natl Acad Sci USA 95:12317–12321
29. **Hosokawa M, Thorens B** 2002 Glucose release from GLUT2-null hepatocytes: characterization of a major and a minor pathway. Am J Physiol 282:E794–E801
30. **Burcelin R, Dolci W, Thorens B** 2000 Portal glucose infusion in the mouse induces hypoglycemia. Evidence that the hepatoportal glucose sensor stimulates glucose utilization. Diabetes 49:1635–1642
31. **Somogyi M** 1945 Determination of blood sugar. J Biol Chem 160:69–73
32. **Foretz M, Pacot C, Dugail I, Lemarchand P, Guichard C, Le Liepvre X, Berthelier-Lubrano C, Spiegelman B, Kim JB, Ferre P, Foufelle F** 1999 ADD1/SREBP-1c is required in the activation of hepatic lipogenic gene expression by glucose. Mol Cell Biol 19:3760–3768
33. **Kliewer SA, Forman BM, Blumberg B, Ong ES, Borgmeyer U, Mangelsdorf DJ, Umesono K, Evans RM** 1994 Differential expression and activation of a family of murine peroxisome proliferator-activated receptors. Proc Natl Acad Sci USA 91:7355–7359
34. **Gremlich S, Nolan C, Roduit R, Burcelin R, Peyot ML, Delghingaro-Augusto V, Desvergne B, Michalik L, Prentki M, Wahli W** 2005 Pancreatic islet adaptation to fasting is dependent on peroxisome proliferator-activated receptor α transcriptional up-regulation of fatty acid oxidation. Endocrinology 146: 375–382
35. **Xu J, Xiao G, Trujillo C, Chang V, Blanco L, Joseph SB, Bassilian S, Saad MF, Tontonoz P, Lee WN, Kurland IJ** 2002 Peroxisome proliferator-activated receptor α (PPARα) influences substrate utilization for hepatic glucose production. J Biol Chem 277:50237–50244
36. **Gnudi L, Shepherd PR, Kahn BB** 1996 Over-expression of GLUT4 selectively in adipose tissue in transgenic mice: implications for nutrient partitioning. Proc Nutr Soc 55:191–199
37. **Tozzo E, Gnudi L, Kahn BB** 1997 Amelioration of insulin resistance in streptozotocin diabetic mice by transgenic overexpression of GLUT4 driven by an adipose-specific promoter. Endocrinology 138:1604–1611
38. **Xu J, Storer PD, Chavis JA, Racke MK, Drew PD** 2005 Agonists for the peroxisome proliferator-activated receptor-α and the retinoid X receptor inhibit inflammatory responses of microglia. J Neurosci Res 81:403–411
39. **Postic C, Leturque A, Rencurel F, Printz RL, Forest C, Granner DK, Girard J** 1993 The effects of hyperinsulinemia and hyperglycemia on GLUT4 and hexokinase II mRNA and protein in rat skeletal muscle and adipose tissue. Diabetes 42:922–929
40. **Burcelin R, Kande J, Ricquier D, Girard J** 1993 Changes in uncoupling protein and GLUT4 glucose transporter expressions in interscapular brown adipose

tissue of diabetic rats: relative roles of hyperglycaemia and hypoinsulinaemia. Biochem J 291:109–113
41. **Rosen ED, Sarraf P, Troy AE, Bradwin G, Moore K, Milstone DS, Spiegelman BM, Mortensen RM** 1999 PPARγ is required for the differentiation of adipose tissue *in vivo* and *in vitro*. Mol Cell 4:611–617
42. **Auwerx J** 1999. PPARγ, the ultimate thrifty gene. Diabetologia 42:1033–1049
43. **Dalen KT, Ulven SM, Bamberg K, Gustafsson JA, Nebb HI** 2003 Expression of the insulin-responsive glucose transporter GLUT4 in adipocytes is dependent on liver X receptor α. J Biol Chem 278:48283–48291
44. **Braissant O, Foufelle F, Scotto C, Dauca M, Wahli W** 1996 Differential expression of peroxisome proliferator-activated receptors (PPARs): tissue distribution of PPAR-α, -β, and -γ in the adult rat. Endocrinology 137:354–366
45. **Chesnokova V, Melmed S** 2002 Minireview: neuro-immuno-endocrine modulation of the hypothalamic-pituitary-adrenal (HPA) axis by gp130 signaling molecules. Endocrinology 143:1571–1574
46. **Obici S, Feng Z, Tan J, Liu L, Karkanias G, Rossetti L** 2001 Central melanocortin receptors regulate insulin action. J Clin Invest 108:1079–1085
47. **Burcelin R, Uldry M, Foretz M, Perrin C, Dacosta A, Nenniger-Tosato M, Seydoux J, Cotecchia S, Thorens B** 2004 Impaired glucose homeostasis in mice lacking the α1b-adrenergic receptor subtype. J Biol Chem 279:1108–1115
48. **Obici S, Rossetti L** 2003 Nutrient sensing and the regulation of insulin action and energy balance. Endocrinology 144:5172–5178
49. **Obici S, Feng Z, Arduini A, Conti R, Rossetti L** 2003 Inhibition of hypothalamic carnitine palmitoyltransferase-1 decreases food intake and glucose production. Nat Med 9:756–761
50. **Liu L, Karkanias GB, Morales JC, Hawkins M, Barzilai N, Wang J, Rossetti L** 1998 Intracerebroventricular leptin regulates hepatic but not peripheral glucose fluxes. J Biol Chem 273:31160–31167
51. **Sainsbury A, Cusin I, Doyle P, Rohner-Jeanrenaud F, Jeanrenaud B** 1996 Intracerebroventricular administration of neuropeptide Y to normal rats increases obese gene expression in white adipose tissue. Diabetologia 39: 353–356
52. **Li G, Zhang Y, Wilsey JT, Scarpace PJ** 2005 Hypothalamic pro-opiomelanocortin gene delivery ameliorates obesity and glucose intolerance in aged rats. Diabetologia 48:2376–2385

***Endocrinology* is published monthly by The Endocrine Society (http://www.endo-society.org), the foremost professional society serving the endocrine community.**